Geosci. Model Dev. Discuss., https://doi.org/10.5194/gmd-2018-231
Manuscript under review for journal Geosci. Model Dev.
Discussion started: 15 October 2018

Geoscientific Model Development Discussions

Interactive Impacts of Fire and Vegetation Dynamics on Global Carbon and Water Budgets using Community Land Model version 4.5

Hocheol Seo[1], and Yeonjoo Kim[1]

[1]Department of Civil and Environmental Engineering, Yonsei University, Seoul 03722, Korea.

Correspondence to: Yeonjoo Kim (yeonjoo.kim@yonsei.ac.kr)

Abstract

Fire plays an important role in terrestrial ecosystems. The burning of biomass affects carbon and water fluxes and the distribution of vegetation. To understand the effect of the interactive processes of fire and ecological succession on land surface carbon and water fluxes, this study utilized the Community Land Model version 4.5 to conduct a series of experiments that included and excluded fire and dynamic vegetation processes. Results of the experiments that excluded dynamic vegetation showed a global increase in net ecosystem production (NEP) in post-fire regions, which has been shown in previous studies with the similar modeling practices. However, inclusion of dynamic vegetation revealed a fire-induced decrease in NEP in some regions. Additionally, the carbon sink in post-fire regions reduced when the dominant vegetation type was changed from trees to grasses. This study shows that inclusion of dynamic vegetation enhances carbon emissions from fire by reducing terrestrial carbon sinks; however, this effect is somewhat mitigated by the increase in terrestrial carbon sinks when dynamic vegetation is not used. Results also show that fire-induced changes in vegetation modify the soil moisture profile because grasslands are more dominant in post-fire regions; this results in less moisture within top soil layers compared to non-burned regions, even though transpiration is reduced overall. These findings are different from those of previous fire model evaluations, that ignore vegetation dynamics, and thus highlight the importance of interactive processes between fire and vegetation dynamics, particularly when evaluating recent model developments with respect to fire and vegetation dynamics.

Keywords

Fire model, Dynamic vegetation model, Terrestrial carbon balance, Community Land Model, Terrestrial water balance

Geosci. Model Dev. Discuss., https://doi.org/10.5194/gmd-2018-231
Manuscript under review for journal Geosci. Model Dev.
Discussion started: 15 October 2018

Geoscientific Model Development Discussions

1 Introduction

Wild fire is a natural process that influences ecosystems and carbon and water cycles worldwide (Gorham, 1991; Bowman et al., 2009; Harrison et al., 2010). Climate and vegetation control both the occurrence of fire and its spread, which in turn affects climate and vegetation (Vilà et al., 2001; Balch et al., 2008), and when fire destroys forests and grasslands the distribution of vegetation is affected (Clement & Touffet, 1990; Rull, 1999). Fire causes the formation of trace gases and aerosols, which are important elements in the radiative balance of the atmosphere (Scholes et al., 1996; Fiebig et al., 2003); aerosols can affect surface air temperature, precipitation, and circulation (Tarasova et al., 1999; Lau & Kim, 2006; Andreae & Rosenfeld, 2008).

Changes in soil properties occur in regions affected by fire, and leaves and roots can be annihilated in such regions (Noble et al., 1980; Swezy & Agee, 1991). Each year, fire transports approximately 2.1 Pg of carbon from soil and vegetation into the atmosphere in the form of carbon dioxide and other carbon compounds (van der Werf et al., 2010). Harden et al. (2000) postulated that approximately 10–30% of annual net primary productivity (NPP) disappeared through fires in upland forests. In addition, transpiration and canopy evaporation decreases due to the reduction in leaf numbers (Clinton et al., 2011; Beringer et al., 2015). Soil has also been found to develop a water repellent layer during fire, which is attributed to intense heating (DeBano, 1991), and the ash produced by biomass combustion can impact the quality of runoff (Townsend & Douglas, 2000).

In post-fire regions, plant distribution gradually changes over time from bare ground to grassland, shrubland, and finally to forest during the process of ecological succession (Prach & Pyšek, 2001). In this respect, the structure and distribution of vegetation can be altered by fire in post-fire regions (Wardle et al., 1997); for example, several studies have suggested that the existence of grass and trees in the savanna can be attributed to fire (Hochberg et al., 1994; Sankaran et al., 2004; Baudena et al., 2010). However, fire can also wipe out succession.

Fire affects many different aspects of the Earth system. Therefore, a certain degree of process-based representation of fire is included in Earth system models, such as within dynamic global vegetation models (DGVMs), land surface models (LSMs), and Earth system models (ESMs; Rabin et al., 2017). Studies have applied fire models to global climate models to investigate the occurrence and spread of fire and how it impacts climate and vegetation (e.g., Pechony & Shindell, 2010; Li et al., 2012; 2013). For example, Bond et al. (2005) used the Sheffield DGVM (SDGVM) and performed the first global study on the extent to which fire determines global vegetation patterns by preventing ecosystems from achieving potential height, biomass, and dominant functional types expected under an ambient climate (i.e., potential vegetation).

In recent years, global fire models have grown in complexity (Hantson et al., 2016), and different fire models parameterize different impact factors such as fuel moisture, fuel size, the probability of lightning, and human effects. In this respect, the Fire Model Intercomparison Project (FireMIP) evaluated the strength and weakness of each fire model by comparing the performance of different fire models and suggesting improvements for individual models (Rabin et al., 2017).

A process-based fire parameterization of intermediate complexity known as the Community Earth System Model (CESM) has been developed and assessed within the framework of the National Center for Atmospheric Research (NCAR) (Li et al., 2012; 2013; 2014), and the latest satellite-based Global Fire Emission Database version

Geosci. Model Dev. Discuss., https://doi.org/10.5194/gmd-2018-231
Manuscript under review for journal Geosci. Model Dev.
Discussion started: 15 October 2018

3 (GFED3), which is derived from moderate resolution imaging spectroradiometer (MODIS) fire count products, has been used to improve fire parameterizations. Furthermore, the impact of fire on carbon, water, and energy balances has also been investigated within the CESM framework (Li et al., 2014; Li & Lawrence, 2017). However, although these studies have considered land-atmosphere interactions with CLM coupled to the atmospheric model, they have ignored changes in global vegetation patterns due to fire processes, even though the initial model developed by Li et al., (2012) was designed to consider vegetation dynamics (i.e., changes in vegetation distribution) within the Community Land Model (CLM)-DGVM.

It is important to understand the possible influences of fire processes on water and carbon exchanges and vegetation distribution, and their combined effects; however, few studies to date have assessed this complicated global process. Therefore, in this study, we aim to understand the interactive effects of fire and ecological succession on carbon and water fluxes at the land's surface. Specifically, we conduct a series of numerical experiments using the NCAR CLM that variously include and exclude fire and dynamic vegetation processes. Our results show that the impact of fire on carbon and water balances (especially in net ecosystem production (NEP) and soil moisture) on ecological succession is different from that on static vegetation.

2 Model and Experimental Design

2.1 Model description

This study used CLM version 4.5, which is the land model of NCAR CESM version 1.2 The CESM is maintained by NCAR's Climate Global Dynamics Laboratory (CGD), and it comprises different components such as land, atmosphere, ocean, land ice, and ocean ice (Worley at el., 2011; Kay et al., 2012). Each component utilizes various formulae to represent the complex interplay of physical, chemical, and biological processes, and each can be used either independently or coupled (Smith et al., 2010; Neale et al., 2012; Bonan et al., 2013). Land surface in the CLM is represented by sub-grid land cover (glacier, lake, wetland, urban, or vegetated), and vegetation coverage is represented by 17 plant functional types (PFTs) comprising 11 tree PFTs, two crop PFTs, three grass PFTs, and bare ground. For a detailed description of the model, please refer to Lawrence et al. (2011).

In this study, CLM 4.5 was extended using the biogeochemistry (BGC) model option; this configuration simulates the carbon and nitrogen cycles in addition to biophysics and hydrology (Paudel et al., 2016). In CLM with BGC, the spatial distribution of PFTs is set using monthly climatological satellite data (Lawrence & Chase, 2007), which differs between months but not between years. Climatological PFT data are conserved based on MODIS and Advanced Very High-Resolution Radiometer data. Land fractions are divided into bare ground, grass, shrub, and evergreen/deciduous tree types. In addition, grass, shrub, and tree PFTs are classified into tropical, temperate, and boreal types, based on the physiology and climate rules of Nemani et al. (1996). Vegetation is further divided into C3 or C4 plants based on MODIS derived leaf area index (LAI) values and the mapping methods of Still et al. (2003).

Certain BGC simulations were run using dynamic vegetation (DV; BGC-DV), which can simulate biogeographical changes in the natural vegetation distribution and mortality processes (Castillo et al., 2012; 2013).

Geosci. Model Dev. Discuss., https://doi.org/10.5194/gmd-2018-231
Manuscript under review for journal Geosci. Model Dev.
Discussion started: 15 October 2018

However, other BGC simulations did not employ the DV option (hereafter, BGConly). In BGC-DV simulations, a PFT can occupy a region or degenerate by competing with other PFTs, or they can coexist under various environmental factors, such as light, soil moisture, temperature, and fire (Zeng, 2010; Song & Zeng, 2013). In BGConly, whole-plant mortality is parameterized by assuming an annual mortality rate of 2%. Conversely, plant mortality in BGC-DV is determined by heat stress, fire, and growth efficiency (Rauscher et al., 2015).

In the fire model (Li et al., 2012, 2013; Bonan et al., 2013), fire is divided into four sections: non-peat fires outside cropland and tropical closed forests, agricultural fires, deforestation fires in tropical closed forests, and peat fires. Fire counts are determined based on natural and artificial ignitions, fuel availability, fuel combustibility, and anthropogenic and unsuppressed natural fires related to socioeconomic conditions, and the burned area is calculated by multiplying the fire count with the average fire spread, which is considered to be driven by wind speed, PFT, fuel wetness, and socioeconomic influences. In other words, the burning and spread of fire are related to the CLM input parameters of climate and weather conditions, vegetation conditions, socioeconomic conditions, and population density.

Once the burned area is identified, fire impacts, including vegetation mortality, peat burning, and the carbon cycle, can be addressed. For example, the amount of carbon emitted from the fire (E) is calculated as follows,

$$E = A \cdot C \cdot CC, \quad (1)$$

where A is the burned area; C is a vector with elements including the carbon density of the leaf stem and root, and transfer and storage of carbon; and CC is the corresponding combustion completeness factor vector. When the DV option is included in the model, individual plants are killed by fire. The number of PFT individuals killed by fire ($P_{distrub}$) is calculated by,

$$P_{distrub} = \frac{A_b}{f A_g} P\, \xi, \quad (2)$$

where P is the population density for each PFT, ξ is the whole-plant mortality factor for each PFT, A_g is the grid cell area, A_b is the burned area of each PFT, and f is the fraction of coverage of each PFT.

The terrestrial carbon balance is affected when biomass is burned. In this respect, the net ecosystem exchange (NEE) can be estimated using NEP and carbon loss due to biomass burning (C_{fe}) as follows,

$$NEE = -NEP + C_{fe}, \quad (3)$$

2.2 Experimental design

A series of global numerical experiments were conducted for this study using a spatial resolution of 1.9° longitude × 2.5° latitude. Global climate data from the Climate Research Unit (CRU)-National Centers for Environmental Prediction (NCEP) reanalysis were used for atmospheric driving forcing of CLM. Data from 1901 to 2000 included 6-h precipitation, air temperature, wind speed, specific humidity, longwave radiation, and shortwave radiation ranging. Figure 1 summarizes the experimental process used in this study. Initial conditions for the 1850 equilibrium state were provided by NCAR and used to simulate the 20th century transient run. The amount of atmospheric carbon dioxide has increased since the onset of the Industrial Revolution in 1850, and the composition of land cover and vegetation

Geosci. Model Dev. Discuss., https://doi.org/10.5194/gmd-2018-231
Manuscript under review for journal Geosci. Model Dev.
Discussion started: 15 October 2018

have changed (Vitousek et al., 1997; Pitman et al., 2004). Therefore, these changes need to be reflected when running a 20th century transient simulation, and the final surface conditions should represent those of the year 2000 after running the transient simulation using the CLM-BGC model.

Using the simulated surface conditions for 2000, four different 200-y equilibrium CLM simulations (BGConly and BGC-DV simulations with and without the fire model) were conducted, as shown in Table 1. For BGConly runs, a restart file from the transient run was used with and without the fire model (hereafter, BGConly-F and BGConly-NF, respectively). Similarly, the BGC-DV runs were performed using the same restart file to simulate the potential vegetation in 200-y offline BGC-DV runs both with and without the fire model (hereafter, BGC-DV-F and BGC-DV-NF, respectively; Erfanian et al., 2016). In these simulations, the initial global land state was bare ground (there were no plants) and soil conditions, such as soil moisture and temperature, were adjusted to those of the year 2000 (Qiu & Liu, 2016; Wang et al., 2016). While the fire model is optional when using CLM with the BGC, it is always run when using CLM with BGC-DV. Hence, the model was modified when conducting the BGC-DV-NF run, and the burned area was set to equal zero to ignore any incidences of fire.

A comparison between the BGConly-F and BGConly-NF runs enables isolation of the impact of fire on the land's surface, regardless of DV. In addition, the impact of fire and the interactive impact of fire and the distribution of vegetation on the Earth's system can be identified by comparing BGC-DV-F and BGC-DV-NF runs. It is important to remember here that this study focuses on the impact of fire and vegetation dynamics on land carbon and water fluxes by forcing the CLM with the CRU-NCEP climate data (1991–2000) without consideration of land-atmosphere feedbacks. Simulations were run for 200-y from the initial surface conditions of 2000 to derive potential land surface conditions. In addition, the average surface conditions of the last 30-y were compared with the results of simulations, and an analysis of this is presented in the following section.

3 Results and Discussions

3.1 Burned area

The simulated burned area from the BGC-DV-F and BGConly-F runs were compared to the GFED3 dataset, which is a reanalyzed dataset derived from MODIS (Giglio et al., 2013). While GFED3 suggests a global burned area estimate of 380 Mha/year for 1999 to 2011, the BGC-DV-F and BGConly-F runs show burned areas of 320 and 487 Mha/year, respectively. Although these are comparable with GFED3, they are not identical because the model estimate run using CRU-NCEP forcing is a 30-y average of the potential vegetation. In addition, agricultural fires are excluded in BGC-DV-F, as it only simulates natural vegetation (Castillo et al., 2012).

It is apparent that BGC-DV-F estimates the GFED3 burned area more accurately than BGConly-F, and this could be attributed to the fact that the fire model of Li et al. (2012) was originally developed using a comparison of BGC-DV-F CLM simulations with GFED3. In a previous study using a BGC-F type simulation coupled to CAM (Li & Lawrence, 2017), the annual burned area was found to be 489 Mha, which is similar to that of BGConly-F (487 Mha).

Geosci. Model Dev. Discuss., https://doi.org/10.5194/gmd-2018-231
Manuscript under review for journal Geosci. Model Dev.
Discussion started: 15 October 2018

Geoscientific Model Development Discussions

Spatial distributions of burned areas are compared in Figure 2. Compared to GFED3, both BGConly-F and BGC-DV-F runs overestimate the burned area in the Americas and in Asia, while BGC-DV-F also underestimates the burned area in Africa and Oceania. These results can be attributed to the differences between BGC-DV-F and BGConly-F vegetation distributions, as shown in Figure 3 (where PFTs, excluding two crop PFTs, are simplified into six vegetation groups; broadleaf evergreen trees, needleleaf evergreen trees, deciduous trees, shrubs, grasses, and bare ground) (Rauscher et al 2015). In BGC-DV-F (Figure 3a), evergreen and deciduous trees show limited growth whereas grasses and bare ground predominate in regions such as southern Africa. Overall, BGC-DV-F simulates trees on 37.5% of the global land area; however, observations (Figure 3b) indicate that trees cover 41.46% (Table 2). However, more trees provide increased fuel for the occurrence and spread of fire in BGC-DV-F compared to BGConly-F

3.2 Interactions between vegetation and fire processes

In this section, we assess the impact of fire processes on the distribution of vegetation by comparing BGC-DV-F and BGC-DV-NF simulations (Table 2 and Figures 3 and 4). Figure 4 shows the vegetation distribution of BGC-DV-NF and BGC-DV-F minus BGC-DV-NF; difference plots clearly indicate large differences in vegetation cover in areas of high fire frequency (i.e., South Africa, South America, western North America, India, and a portion of China), as shown in Table 2, whereas areas with relatively low fire occurrence (i.e., the Arctic and desert regions) show small differences.

The relationship between vegetation distribution and fire occurrence is investigated by estimating the fraction of burned areas (Figure 5), where fractions are grouped into four categories (>10%, 10%~1%, 1%~0.1% and, <0.1%) for each vegetation type, and they illustrate a nonlinear change in vegetation distribution in response to post-fire area. Changes in the vegetation distribution are small in areas with minimal fire occurrence or where the burned area fraction is small (0.1~1%). However, relatively large changes in vegetation distribution are apparent when the burned area fraction exceeds 1%. Furthermore, there are large changes in the vegetation distribution in areas with burned area fractions above 10%, including increases in bare ground, grass, and shrubs (31.19, 52.28, and 7.91%, respectively) but decreases in deciduous, needleleaf evergreen, and broadleaf evergreen trees (8.85, 79.22, and 91.17%, respectively).

Areas that experience a higher frequency of fire occurrence have larger vegetation distribution differences, which suggests that fire has an influence on vegetation mortality. In ecological processes, plants die in regions where fire occurs; grasses with rapid growth rates then occupy regions after fire. Therefore, fire increases the ratios of bare ground and grassland but reduces the percentage number of trees. However, there are no marked changes in the fractions of shrubs and deciduous trees in the middle of the ecological succession process with respect to the presence or absence of fire (Table 2). When fire occurs in a region where shrubs grow, the ratio of shrubland is diminished, but fire increases the ratio of shrubland in regions where trees may evolve from shrubs. In the same way as shrubs, the deciduous trees are increased or decreased due to fire. Thus, it is apparent that the role of fire in areas of shrubland and deciduous trees differs according to the region, and the actual vegetation distribution is a result of complicated factors that include fire, climate, topography, and soil conditions (He et al., 2007; Cimalová & Lososová, 2009).

Geosci. Model Dev. Discuss., https://doi.org/10.5194/gmd-2018-231
Manuscript under review for journal Geosci. Model Dev.
Discussion started: 15 October 2018

Geoscientific Model Development Discussions

204 **3.3 Fire impact on carbon balances**

205 The direct and indirect impacts of fire on carbon balances were investigated by exploring the difference between fire
206 impact when using state and dynamic vegetation (Figure 6 and Table 3). The impact of fire in two cases (BGConly-F
207 minus BGConly-NF (BGCOnly) and BGC-DV-F minus BGC-DV-NF (BGC-CV) were estimated by averaging the
208 final 30-y of each 200-y simulation.

209 Carbon emissions due to fire (direct impacts) are shown in Figure 6. The spatial distributions of the BGConly
210 and BGC-DV runs are similar, but average annual emissions are higher in BGConly (3.4 Pg) compared to BGC-DV
211 (3.0 Pg). This result could be attributed to trees being less dominant in BGC-DV compared to BGConly, which thus
212 causes a reduced fuel load.

213 We note that estimates of carbon emissions from BGConly and BGC-DV are relatively high; however, they
214 do fall within the range of previous findings. For example, 1999–2011 GFED3 data estimated annual direct carbon
215 emissions as being approximately 2.0 Pg. Furthermore, Mouillot et al. (2006) estimated annual carbon emissions as
216 being approximately 3.0 Pg for the end of 20th century and approximately 2.5 Pg for the 20th century average; and Li
217 et al. (2014) and Yue et al. (2015) both estimated 20th century emissions as being 1.9 Pg C yr^{-1} using the CLM4.5 and
218 ORCHIDE land surface models, respectively.

219 In addition to direct carbon emissions, fire influences terrestrial carbon sinks by impacting ecosystem
220 processes, as shown in Figure 6. Fire increases the NEP in post-fire regions in BGConly simulations, which is
221 consistent with the findings of previous studies (Li et al., 2014). However, the overall NEP decrease is 2.5 Pg C y^{-1} in
222 this study, which is greater than the value of 1.9 Pg C yr^{-1} determined by Li et al. (2014). However, Li et al. (2014)
223 performed a transient simulation from 1850 to 2004, whereas the BGConly runs in our study were conducted following
224 an equilibrium simulation using 2000 as the reference year, which thus meant that no fire exchanges were due to land
225 cover changes.

226 Simulations that ignore vegetation dynamics (i.e., the BGConly runs in this study; Li et al., 2014; Yue et al.,
227 2015) show a global fire-induced NEP increase when comparing fire-on and fire-off runs. However, a decrease in fire-
228 induced NEP is apparent in some regions when using BGC-DV (Figure 6). This carbon sink reduction occurs in
229 regions where dominant PFTs changed from broadleaf and needleleaf evergreen trees to grasses (as shown in Table 3
230 and Figure 6). Table 4 shows the correlation coefficients between percentage changes in vegetation types and changes
231 in carbon fluxes (NEP, NPP, and heterotrophic respiration (Rh)) for six different PFTs in each grid cell), and Figure
232 7 shows the broadleaf evergreen tree, needleleaf evergreen tree, and grass PFTs. It is apparent that NEP changes are
233 strongly linked to changes in the dominant PFTs; for example, decreases in broadleaf evergreen and needleleaf
234 evergreen trees, and increases in grasses. Furthermore, associations between changes in NEP and PFTs are related to
235 changes in both NPP and Rh to some extent. Our results differ from those of previous studies that did not consider
236 vegetation dynamics (e.g., Amiro et al., 2010), because the inclusion of vegetation dynamics enables the model to
237 capture NEP decreases in post-fire regions at the beginning of post fire-succession.

238 As land use change is not considered in this study, the overall impact of fire was estimated by the sum of
239 carbon emissions and terrestrial carbon sinks (Eq. 3). Both simulations resulted in carbon sources in the post-fire
240 regions, even though different processes were involved. Although carbon emissions due to fire were partly negated

Geosci. Model Dev. Discuss., https://doi.org/10.5194/gmd-2018-231
Manuscript under review for journal Geosci. Model Dev.
Discussion started: 15 October 2018

by the increased terrestrial carbon sinks in the BGConly runs, they were enhanced by the reduction in terrestrial carbon sinks in the BGC-DV runs.

3.4 Fire impact on water balances

The impact of fire on the water balance was examined by estimating changes in runoff, evapotranspiration, and soil moisture, and by making a comparison between BGConly and BGC-DV (Table 5 and Figure 8). Increases in runoff and decreases in evapotranspiration (ET) were found in post-fire regions to different degrees, which is consistent with the results of previous studies (Neary et al., 2005; Li & Lawrence, 2017). Our study used CLM as a standalone model without coupling to the atmospheric or ice models, whereas Li and Lawrence (2017) examined the impact of fire on the global water budget using CLM-BGC coupled with the CAM and CICE models and found that the impact of fire on global annual precipitation was limited.

Li and Lawrence (2017) pointed out that a reduction in the vegetation canopy (LAI; Table 6) is a critical pathway for fire impacting on ET and leading to its decrease. Fire events lower the leaf area, which decreases vegetation transpiration and canopy evaporation; however, they also expose more of the soil to the air and sunlight, which increases soil evaporation. Post-fire decreases in vegetation height (Table 6) can both increase and decrease ET, as the resulting decrease in land surface roughness potentially reduces water and energy exchanges and leads to higher leaf temperatures and wind speeds. In this study, both BGConly and BGC-DV runs show the vegetation canopy is the main pathway leading to ET decrease, which is similar to the findings of Li and Lawrence (2017). In addition, an examination of how changes in the vegetation composition within post-fire regions influences the above mechanisms shows that overall impacts of ET and runoff do not differ greatly when dynamic vegetation is employed by the model. However, results show that fire-induced vegetation changes (from trees to grass or bare ground) in BGC-DV lead to a marked decrease in canopy transpiration and increased soil evaporation relative to BGConly. Fire destroys plant roots and leaves, and changes in the dominant vegetation types in BGC-DV lead to changes in the soil moisture profile through reduced transpiration (Figure 9 and Table 7). Consequently, there is less water stress in each soil layer within burned areas than in non-burned areas. Grasslands dominate in post-fire regions when using BGC-DV, and they absorb and transpire more water from the top soil layer compared to trees (Mazzacavallo & Kulmatiski, 2015). There is thus less moisture in the top soil layers in fire affected regions than in non-burned regions, despite the fact that the overall transpiration is diminished. Put simply, fire has an impact on the vegetation distribution, which in turn impacts the soil water profile.

Changes in ET and runoff do not differ markedly between BGConly and BGC-DV, despite differences in the vegetation canopy and height, and soil moisture. This result could be attributed to the fact that an offline CLM was used, which does not allow for land-atmosphere interactions. We therefore expect that the impact of fire on precipitation would be more significant in BGC-DV than in BGConly because fire directly influences land cover characteristics.

Geosci. Model Dev. Discuss., https://doi.org/10.5194/gmd-2018-231
Manuscript under review for journal Geosci. Model Dev.
Discussion started: 15 October 2018

4. Conclusions

To understand the interplay of vegetation dynamics and fire impacts, we conducted a series of numerical experiments using CLM both with and without fire and dynamic vegetation processes enabled. In particular, we investigated fire influences on vegetation distribution, and how such changes influence terrestrial carbon and water fluxes.

As expected, results showed that fire interrupts the process of ecological succession, which thus impacts the global vegetation distribution. Fire transforms some regions into bare ground, and grasses quickly dominate as they grow faster than trees. For shrubs and deciduous trees in the mid-stages of ecological succession, we found no large differences in the overall coverage ratios between simulations including vegetation dynamics and those that did not. Simulations that did not consider vegetation dynamics showed a fire-induced global increase in NEP; however, a fire-induced decrease in NEP was found in some regions in BGC-DV. We also found a carbon sink reduction in regions where the dominant PFT changed from broadleaf and needleleaf evergreen trees to grasses. While carbon emissions due to fire were partly negated by increased terrestrial carbon sinks (NEP) in BGConly runs, they were enhanced by the reduction in terrestrial carbon sinks in BGC-DV runs when dynamic vegetation was considered.

Fire-induced changes in vegetation from trees to grass or bare ground resulted in a decrease in canopy transpiration and increased soil evaporation in post-fire regions for BGC-DV; however, there were no marked differences in the overall impacts on ET and runoff between simulations that used dynamic vegetation and those that did not. Interestingly, however, changes in dominant vegetation types in BGC-DV led to changes in the soil moisture profile. Furthermore, the increased distribution of grassland cover was more dominant in post-fire regions, which then resulted in less moisture in the top soil layers compared to non-burned areas, despite that fact that transpiration diminished overall.

Enabling the vegetation dynamics module in the CLM assists in gaining an understanding of the interactive impacts of fire and vegetation dynamics. However, uncertainty still exists because of the limited simulated potential vegetation distribution using CLM with BGC-DV-F. Furthermore, the final potential vegetation state of the BGC-DV model did not always correspond to the observed distribution (Figure 3). For example, shrubs in the tundra were found to be rare in both BGC-DV-F and BGC-DV-NF. Furthermore, crops, needleleaf evergreen boreal, and shrub boreal cannot be simulated by the DV module, as noted in previous studies (Zeng et al., 2008).

The fire module in CLM is parameterized to estimate fire occurrence, fire spread, and fire impact. Thresholds used to estimate fuel combustibility are dependent on relative humidity and surface air temperatures; however, these values may not be suitable for all regions (Zhang et al., 2016). In addition, the economic impact of fire occurrence and the socioeconomic impact of fire spread are estimated using the input datasets of population density (person/km^2) and GDP (US$/capita), respectively (Li et al., 2013). Uncertainty due to socioeconomic factors should be noted for both historical and future simulations, because changes in these factors may vary by country (Steelman & Burke, 2006). It is evident that our understanding of fire needs to improve, because fire plays an important role in the distribution of vegetation and in carbon, water, and energy cycling. Furthermore, this study shows that fire models are strongly impacted by vegetation distribution; therefore, fire simulations would improve if improvements were made to the dynamic vegetation model.

312 **Code and Data Availability**

313 The code of and input datasets for CLM are downloaded from the NCAR CLM website (refer to cesm.ucar.edu).
314

315 **Author Contribution**

316 YK and HS designed the study and HS performed the model simulations with processing the data and modifying the
317 code. Both YK and HS analyzed the results and wrote the manuscript.
318

319 **Acknowledgements**

320 This study was supported by the Basic Science Research Program through the National Research Foundation of Korea,
321 which was funded by the Ministry of Science, ICT & Future Planning (2018R1A1A3A04079419), and by the Korea
322 Polar Research Institute (KOPRI, PN17900).
323
324

325 **References**

326
327 Andreae, M. O., and Rosenfeld, D.: Aerosol-cloud-precipitation interactions. Part 1. The nature and sources of cloud-
328 active aerosols, Earth Sci. Rev., 89(1–2), 13–41, doi.org/10.1016/j.earscirev.2008.03.001, 2008.
329 Amiro, B. D., Barr, A. G., Barr, J. G., Black, T. A., Bracho, R., Brown, M., Chen, J., Clark, K. L., Davis, K. J., Desai,
330 A. R., Dore, S., Engel, V., Fuentes, J. D., Goldstein, A. H., Goulden, M. L., Kolb, T. E., Lavigne, M. B., Law, B. E.,
331 Margolis, H. A., Martin, T., McCaughey, J. H., Misson, L., Montes-Helu, M., Noormets, A., Randerson, J. T., Starr,
332 G., and Xiao, J.: Ecosystem carbon dioxide fluxes after disturbance in forests of North America, J. Geophys. Res.-
333 Biogeosci., 115(4), doi.org/10.1029/2010JG001390, 2010.
334 Balch, J. K., Nepstad, D. C., Brando, P. M., Curran, L. M., Portela, O., de Carvalho, O., and Lefebvre, P.: Negative
335 fire feedback in a transitional forest of southeastern Amazonia, Global Change Biol., 14(10), 2276–2287,
336 doi.org/10.1111/j.1365-2486.2008.01655.x, 2008.
337 Baudena, M., D'Andrea, F., and Provenzale, A.: An idealized model for tree-grass coexistence in savannas: The role
338 of life stage structure and fire disturbances, J. Ecol., 98(1), 74–80, doi.org/10.1111/j.1365-2745.2009.01588.x, 2010.
339 Beringer, J., Hutley, L., Abramson, D., Arndt, S., Briggs, P., Bristow, M., Canadell, J., Cernusak, L., Eamus, D.,
340 Edwards, A., Evans, B., Fest, B., Goergen, K., Grover, S., Hacker, J., Haverd, V., Kanniah, K., Livesley, S., Lynch,
341 A., Maier, S., Moore, C., Raupach, M., Russell-Smith, J., Scheiter, S., Tapper, N., and Uotila, P.: Fire in Australian
342 savannas: From leaf to landscape, Global Change Biol., 21(1), 62–81, doi.org/10.1111/gcb.12686, 2015.

343 Bonan, G. B., Drewniak, B., Huang, M., Koven, C. D., Levis., S., Li, F., Riley, W. J., Subin, Z. M., Swenson, S. C.
344 and Thronton, P. E.: Technical Description of Version 4.5 of the Community Land Model (CLM), NCAR/TN-
345 486+STR, NCAR, Boulder, Colo., 2013.
346 Bond, W. J., Woodward, F. I., and Midgley, G. F.: The global distribution of ecosystems in a world without fire, New
347 Phytol., 165(2), 525–538, doi.org/10.1111/j.1469-8137.2004.01252.x, 2005.
348 Bowman, D., Balch, J., Artaxo, P., Bond, W., Carlson, J., Cochrane, M., Antonio, C., Defries, R., Doyle, J., Harrison,
349 S., Johnston, F., Keeley, J., Krawchuk, M., Kull, C., Marston, J., Moritz. M., Prentice,I., Roos, C., Scott, A., Swetnam,
350 T., van der Werf, G., and Pyne, S.: Fire in the Earth System, Science, 324(5926), 481–484,
351 doi.org/10.1126/science.1163886, 2009.
352 Castillo, C. K. G., and Gurney, K. R.: A sensitivity analysis of surface biophysical, carbon, and climate impacts of
353 tropical deforestation rates in CCSM4-CNDV, J. Clim., 26(3), 805–821, doi.org/10.1175/JCLI-D-11-00382.1, 2013.
354 Castillo, C. K. G., Levis, S., and Thornton, P.: Evaluation of the new CNDV option of the community land model:
355 Effects of dynamic vegetation and interactive nitrogen on CLM4 means and variability, J. Clim., 25(11), 3702–3714,
356 doi.org/10.1175/JCLI-D-11-00372.1, 2012.
357 Cimalová, Š., and Lososová, Z.: Arable weed vegetation of the northeastern part of the Czech Republic: Effects of
358 environmental factors on species composition, Plant Ecol., 203(1), 45–57, doi.org/10.1007/s11258-008-9503-1, 2009.
359 Clement, B., and Touffet, J.: Plant Strategies and Secondary Succession on Brittany Heathlands after Severe Fire, J.
360 Veg. Sci., 1(2), 195–202, doi.org/10.2307/3235658, 1990.
361 Clinton, B. D., Maier, C. A., Ford, C. R., and Mitchell, R. J.: Transient changes in transpiration, and stem and soil
362 CO2efflux in longleaf pine (Pinus palustris Mill.) following fire-induced leaf area reduction, Trees – Struct. Funct.,
363 25(6), 997–1007, doi.org/10.1007/s00468-011-0574-6, 2011.
364 DeBano, L.F.: The effects of fire on soil properties, United States Department of Agriculture Forestry Service General
365 Technical Report, INT-2, 151–156., 1991.
366 Erfanian, A., Wang, G., Yu, M., and Anyah, R.: Multimodel ensemble simulations of present and future climates over
367 West Africa: Impacts of vegetation dynamics, J. Adv. Model. Earth Syst., 8(3), 1411–1431,
368 doi.org/10.1002/2016MS000660, 2016.
369 Fiebig, M., Stohl, A., Wendisch, M., Eckhardt, S., and Petzold, A.: Dependence of solar radiative forcing of forest
370 fire aerosol on ageing and state of mixture, Atmos. Chem. Phys. Discuss., 3(2), 1273-1302, doi.org/10.5194/acp-3-
371 881-2003, 2003.
372 Giglio, L., Randerson, J. T., and van der Werf, G. R.: Analysis of daily, monthly, and annual burned area using the
373 fourth-generation global fire emissions database (GFED4), J. Geophys. Res.-Biogeo., 118(1), 317–328,
374 doi.org/10.1002/jgrg.20042, 2013.
375 Gorham, E.: Northern Peatlands : Role in the Carbon Cycle and Probable Responses to Climatic Warming, Ecol. Appl.,
376 1(2), 182–195, doi.org/10.2307/1941811, 1991.
377 Hantson, S., Arneth, A., Harrison, S. P., Kelley, D. I., Prentice, I. C., Rabin, S. S., Archibald, S., Mouillot, F., Arnold,
378 S. R., Artaxo, P., Bachelet, D., Ciais, P., Forrest, M., Friedlingstein, P., Hickler, T., Kaplan, J. O., Kloster, S., Knorr,
379 W., Lasslop, G., Li, F., Mangeon, S., Melton, J. R., Meyn, A., Sitch, S., Spessa, A., van der Werf, G. R., Voulgarakis,

A., and Yue, C.: The status and challenge of global fire modelling, Biogeosciences, 13(11), 3359–3375, doi.org/10.5194/bg-13-3359-2016, 2016.

Harden, J. W., Trumbore, S. E., Stocks, B. J., Hirsch, A., Gower, S. T., O'Neill, K. P., and Kasischke, E. S.: The role of fire in the boreal carbon budget, Global Change Biol., 6(Suppl. 1), 174–184, doi.org/10.1046/j.1365-2486.2000.06019.x, 2000.

Harrison, S.P., Marlon, J.R. and Bartlein, P.J.: Fire in the Earth System, Changing climates, earth systems and society (ed.by J. Dodson), 21–48, Springer, Dordrecht, 2010.

He, M. Z., Zheng, J. G., Li, X. R., and Qian, Y. L.: Environmental factors affecting vegetation composition in the Alxa Plateau, China, J. Arid. Environ., 69(3), 473–489, doi.org/10.1016/j.jaridenv.2006.10.005, 2007.

Hochberg, M. E., Menaut, J. C., and Gignoux, J.: The Influences of Tree Biology and Fire in the Spatial Structure of the West African Savannah, J. Ecol., 82(2), 217-226, doi.org/10.2307/2261290, 1994.

Kay, J. E., Hillman, B. R., Klein, S. A., Zhang, Y., Medeiros, B., Pincus, R., Gettelman, A., Eaton, B., Boyle, J., Marchand, R., and Ackerman, T. P.: Exposing global cloud biases in the Community Atmosphere Model (CAM) using satellite observations and their corresponding instrument simulators, J. Clim., 25(15), 5190–5207, doi.org/10.1175/JCLI-D-11-00469.1, 2012.

Lau, K. M., and Kim, K. M.: Observational relationships between aerosol and Asian monsoon rainfall, and circulation, Geophys. Res. Lett., 33(21), L21810, doi.org/10.1029/2006GL027546, 2006.

Lawrence, D. M., Oleson, K. W., Flanner, M. G., Thornton, P. E., Swenson, S. C., Lawrence, P. J., Zeng, X., Yang, Z., Levis, S., Sakaguchi, K., Bonan., G. B., and Slater, A. G.: Parameterization improvements and functional and structural advances in Version 4 of the Community Land Model, J. Adv. Model. Earth Syst., 3(1), doi.org/10.1029/2011MS00045, 2011.

Lawrence, P. J., and Chase, T. N.: Representing a new MODIS consistent land surface in the Community Land Model (CLM 3.0), J. Geophys. Res.-Biogeo, 112(1), doi.org/10.1029/2006JG000168, 2007.

Li, F., and Lawrence, D. M.: Role of fire in the global land water budget during the twentieth century due to changing ecosystems, J. Clim., 30(6), 1893–1908, doi.org/10.1175/JCLI-D-16-0460.1, 2017.

Li, F., Bond-Lamberty, B., and Levis, S.: Quantifying the role of fire in the Earth system - Part 2: Impact on the net carbon balance of global terrestrial ecosystems for the 20th century, Biogeosciences, 11(5), 1345–1360, doi.org/10.5194/bg-11-1345-2014, 2014.

Li, F., Levis, S., and Ward, D. S.: Quantifying the role of fire in the Earth system - Part 1: Improved global fire modeling in the Community Earth System Model (CESM1), Biogeosciences, 10(4), 2293–2314, doi.org/10.5194/bg-10-2293-2013, 2013.

Li, F., Zeng, X. D., and Levis, S.: A process-based fire parameterization of intermediate complexity in a dynamic global vegetation model, Biogeosciences, 9(7), 2761–2780, doi.org/10.5194/bg-9-2761-2012, 2012.

Mazzacavallo, M. G., and Kulmatiski, A.: Modelling water uptake provides a new perspective on grass and tree coexistence, PLoS ONE, 10(12), e0144300, doi.org/10.1371/journal.pone.0144300, 2015.

Mouillot, F., Narasimha, A., Balkanski, Y., Lamarque, J.-F., and F,eld, C. B.: Global carbon emissions from biomass burning in the 20th century, Geophys. Res. Lett., 33(1), L01801, doi.org/10.1029/2005GL024707, 2006.

417 Neale, R. B., et al.: Description of the NCAR Community Atmosphere Model (CAM5.0), NCAR/TN-486+STR,
418 NCAR, Boulder, Colo., 2012.
419 Neary, D. G. ., Ryan, K. C., and DeBano, L. F.: Wildland Fire in Ecosystems, effects of fire on soil and water, General
420 Technical Report RMRS-GTR-42, 4. U.S. Department of Agriculture, Forest Service, Rocky Mountain Research
421 Station, Ogden, UT., 2005.
422 Nemani, R. R., Running, S. W., Pielke, R. a, and CHase, T. N.: Global vegetation cover changes from coarse resolution
423 satellite data, J. Geophys. Res.-Atmos., 101(D3), 7157–7162, doi.org/Doi 10.1029/95jd02138, 1996.
424 Noble, J. C., Smith, A. W. and Leslie, H. W.: Fire in the mallee shrublands of western New South Wales, Rangeland
425 J., 2(1), 104–114, 1980.
426 Paudel, R., Mahowald, N. M., Hess, P. G. M., Meng, L., and Riley, W. J.: Attribution of changes in global wetland
427 methane emissions from pre-industrial to present using Attribution of changes in global wetland methane emissions
428 from pre-industrial to present using CLM4.5-BGC, Environ. Res. Lett., 11(3), doi:10.1088/1748-9326/11/3/034020,
429 2016.
430 Pechony, O., and Shindell, D. T.: Driving forces of global wildfires over the past millennium and the forthcoming
431 century, PNAS, 107(45), 19167–19170, doi.org/10.1073/pnas.1003669107, 2010.
432 Pitman, A. J., Narisma, G. T., Pielke, R. A., and Holbrook, N. J.: Impact of land cover change on the climate of
433 southwest Western Australia, J. Geophys. Res.-Atmos., 109(D18), D18109, doi.org/10.1029/2003JD004347, 2004.
434 Prach, K., and Pyšek, P.: Using spontaneous succession for restoration of human-disturbed habitats: Experience from
435 Central Europe, Ecol. Eng., 17(1), 55–62, doi.org/10.1016/S0925-8574(00)00132-4, 2001.
436 Qiu, L., and Liu, X.: Sensitivity analysis of modelled responses of vegetation dynamics on the Tibetan Plateau to
437 doubled CO2 and associated climate change, Theor. Appl. Climatol., 124(1–2), 229–239, doi.org/10.1007/s00704-
438 015-1414-1, 2016.
439 Rabin, S. S., Melton, J. R., Lasslop, G., Bachelet, D., Forrest, M. ,Hantson, S., Kaplan, J. O., Li, F., Mangeon, S.,
440 Ward, D. S., Yue, C., Arora, V. K., Hickler, T. ,Kloster, S., Knorr, W., Nieradzik, L., Spessa, A., Folberth, G. A.,
441 Sheehan, T., Voulgarakis, A., Kelley, D. I., Colin Prentice, I., Sitch, S., Harrison, and S., Arneth, A.: The Fire
442 Modeling Intercomparison Project (FireMIP), phase 1: Experimental and analytical protocols with detailed model
443 descriptions, Geosci. Model Dev., 10, 1175-1197, doi.org/10.5194/gmd-10-1175-201, 2017.
444 Rauscher, S. A., Jiang, X., Steiner, A., Williams, A. P., Michael Cai, D., and McDowell, N. G.: Sea surface
445 temperature warming patterns and future vegetation change, J. Clim., 28(20), 7943–7961, doi.org/10.1175/JCLI-D-
446 14-00528.1, 2015.
447 Rull, V.: A palynological record of a secondary succession after fire in the Gran Sabana, Venezuela, J. Quat. Sci.,
448 14(2), 137–152, doi.org/10.1002/(SICI)1099-1417(199903)14:2<137::AID-JQS413>3.0.CO;2-3, 1999.
449 Sankaran, M., Ratnam, J., and Hanan, N. P.: Tree-grass coexstence in savannas revisited - Insights from an
450 examination of assumptions and mechanisms invoked in existing models, Ecol. Lett., 7(6), 480–490,
451 doi.org/10.1111/j.1461-0248.2004.00596.x, 2004.
452 Scholes, R. J., Ward, D. E., and Justice, C. O.: Emissions of trace gases and aerosol particles due to vegetation burning
453 in southern hemisphere Africa, J. Geophys. Res., 101(D19), 23,623-23,682, 1996.

Smith R, et al.: The Parallel Ocean Program (POP) reference manual: Ocean component of the Community Climate System Model (CCSM), Technical Report LAUR-10-01853, Los Alamos National Laboratory, 2010.

Song, X., and Zeng, X.: Investigation of uncertainties of establishment schemes in dynamic global vegetation models, Adv. Atmos. Sci., 31(1), 85–94, doi.org/10.1007/s00376-013-3031-1, 2014.

Steelman, T. A., and Burke, C. A.: Is wildfire policy in the United States sustainable?, J. Forest., 33, 67–72, doi.org/10.2139/ssrn.1931057, 2007.

Still, C. J., Berry, J. A., Collatz, G. J., and DeFries, R. S.: Global distribution of C 3 and C 4 vegetation: Carbon cycle implications, Global Biogeochem. Cycles, 17(1), 6-1-6–14, doi.org/10.1029/2001GB001807, 2003.

Swezy, D. M., and Agee, J. K.: Prescribed-fire effects on fine-root and tree mortality in old-growth ponderosa pine, Can. J. For. Res., 21(5), 626–634, doi.org/10.1139/x91-086, 1991.

Tarasova, T. A., Nobre, C. A., Holben, B. N., Eck, T. F., and Setzer, A.: Assessment of smoke aerosol impact on surface solar irradiance measured in the Rondônia region of Brazil during Smoke, Clouds, and Radiation – Brazil, J. Geophys. Res.-Atmos., 104(D16), 19161–19170, doi.org/10.1029/1999JD900258, 1999.

Townsend, S., and Douglas, M. M.: The effect of three fire regimes on stream water quality, water yield and export coefficients in a tropical savanna (Northern Australia), J. Hydrol., 229, 118–137, 2000.

Van der Werf, G. R., Randerson, J. T., Giglio, L., Collatz, G. J., Mu, M., Kasibhatla, P. S., Morton, D. C., DeFries, R. S., Jin, Y., and van Leeuwen, T. T.: Global fire emissions and the contribution of deforestation, savanna, forest, agricultural, and peat fires (1997–2009), Atmos. Chem. Phys., 10, 11707–11735, 2010.

Vilà, M., Lloret, F., Ogheri, E., and Terradas, J.: Positive fire-grass feedback in Mediterranean Basin woodlands, For. Ecol. Manage., 147, 3–14. 2001.

Vitousek, P. M., Mooney, H. a, Lubchenco, J., and Melillo, J. M.: Human Domination of Earth' s Ecosystems, Science, 277(5325), 494–499, doi.org/10.1126/science.277.5325.494, 1997.

Wang, G., Yu, M., Pal, J. S., Mei, R., Bonan, G. B., Levis, S., and Thornton, P. E.: On the development of a coupled regional climate–vegetation model RCM–CLM–CN–DV and its validation in Tropical Africa, Clim. Dyn., 46(1–2), 515–539, doi.org/10.1007/s00382-015-2596-z, 2016.

Wardle, D., Olle, Z., Greger, H., and Gallet, C.: The Influence of Island Area on Ecosystem Properties The Influence of Island Area on Ecosystem Properties, Science, 277(5330), 1296–1300, doi.org/10.1126/science.277.5330.1296, 1997.

Worley, P. H., Mirin, A. A., Craig, A. P., Taylor, M. A., Dennis, J. M., and Vertenstein, M.: Performance of the community earth system model, in: High Performance Computing, Networking, Storage and Analysis (SC), 2011 International Conference, Seattle, WA, 2011.

Yue, C., Ciais, P., Cadule, P., Thonicke, K., and Van Leeuwen, T. T.: Modelling the role of fires in the terrestrial carbon balance by incorporating SPITFIRE into the global vegetation model ORCHIDEE -Part 2: Carbon emissions and the role of fires in the global carbon balance, Geosci. Model Dev., 8(5), 1321–1338, doi.org/10.5194/gmd-8-1321-2015, 2015.

Zeng, X.: Evaluating the dependence of vegetation on climate in an improved dynamic global vegetation model, Adv. Atmos. Sci., 27(5), 977–991, 2010.

Geosci. Model Dev. Discuss., https://doi.org/10.5194/gmd-2018-231
Manuscript under review for journal Geosci. Model Dev.
Discussion started: 15 October 2018

491 Zeng, X., Zeng, X., and Barlage, M.: Growing temperate shrubs over arid and semiarid regions in the Community
492 Land Model-Dynamic Global Vegetation Model, Global Biogeochem. Cycles, 22(3), GB3003,
493 doi.org/10.1029/2007GB003014, 2008.
494 Zhang, L., Mao, J., Shi, X., Ricciuto, D., He, H., Thornton, P., Yu, G., Li, P., Liu, M., Ren, X., Han, S., Li, Y., Yan,
495 J., Hao, Y., and Wang, H.: Evaluation of the Community Land Model simulated carbon and water fluxes against
496 observations over ChinaFLUX sites, Agric. For. Meteorol., 226–227, 174–185,
497 doi.org/10.1016/j.agrformet.2016.05.018, 2016.
498
499

Geosci. Model Dev. Discuss., https://doi.org/10.5194/gmd-2018-231
Manuscript under review for journal Geosci. Model Dev.
Discussion started: 15 October 2018

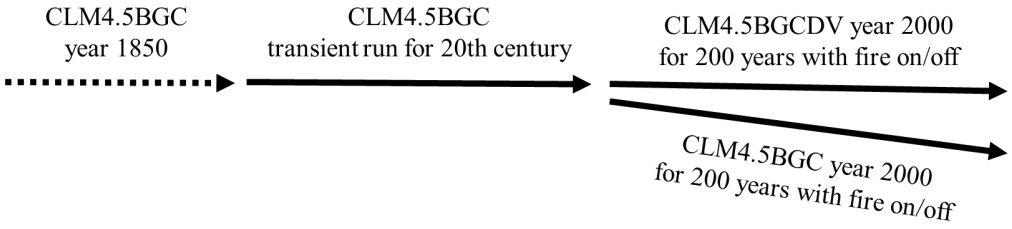

500
501

502 **Figure 1:** Flowchart showing model simulations conducted to investigate the interactive impact of fire and ecological succession
503 on the Earth system using Community Land Model (CLM4.5) simulations extended with biogeochemistry (CLM4.5BGC) and
504 BGC with dynamic vegetation (CLM4.5BGCDV).

505
506

Geosci. Model Dev. Discuss., https://doi.org/10.5194/gmd-2018-231
Manuscript under review for journal Geosci. Model Dev.
Discussion started: 15 October 2018

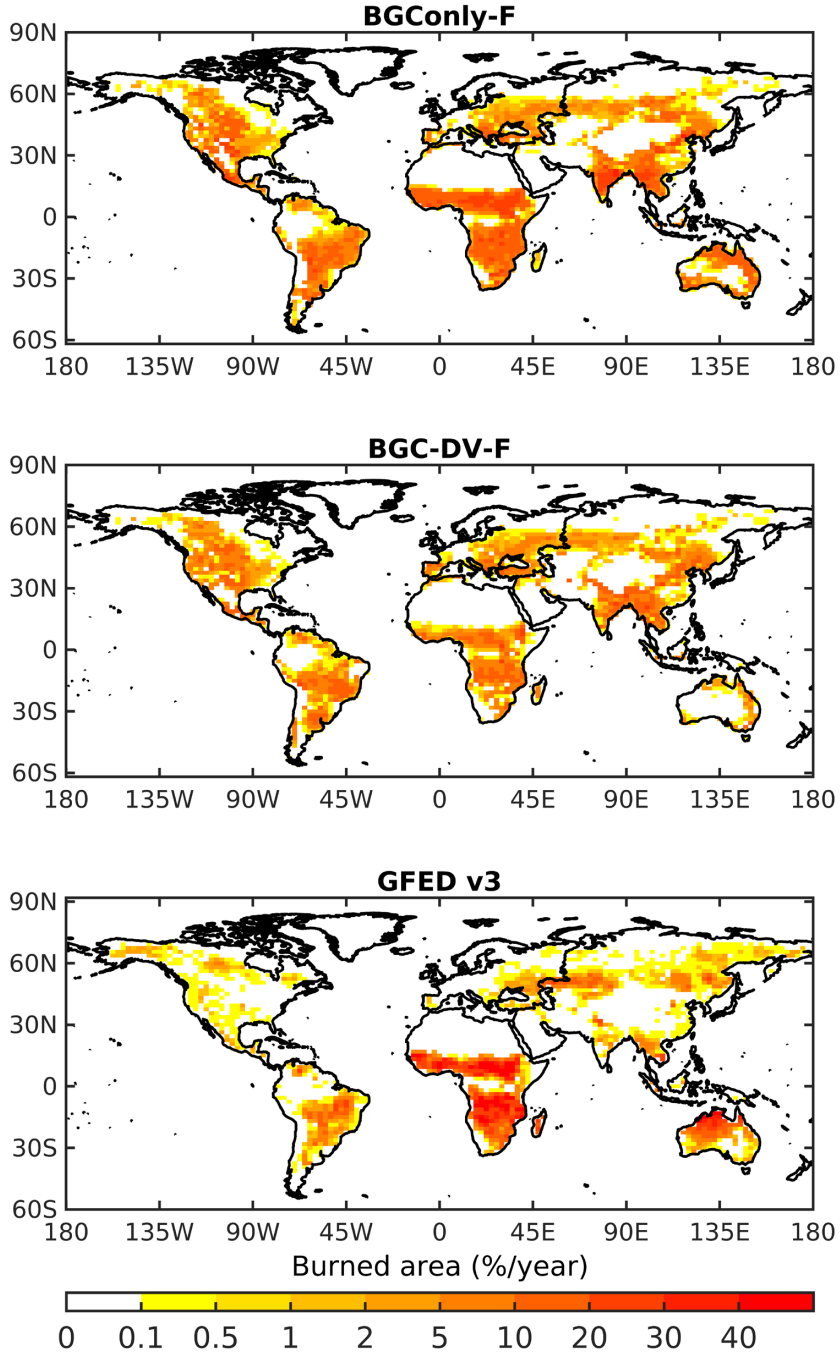

507

508 **Figure 2:** Annual burned area percentage by grid cell for CLM4.5BGC with fire (BGConly-F), CLM4.5BGCDV with fire (BGC-
509 DV-F), and Global Fire Emission Database version 3 (GFED v3).

510 .

Geosci. Model Dev. Discuss., https://doi.org/10.5194/gmd-2018-231
Manuscript under review for journal Geosci. Model Dev.
Discussion started: 15 October 2018

Geoscientific Model Development Discussions

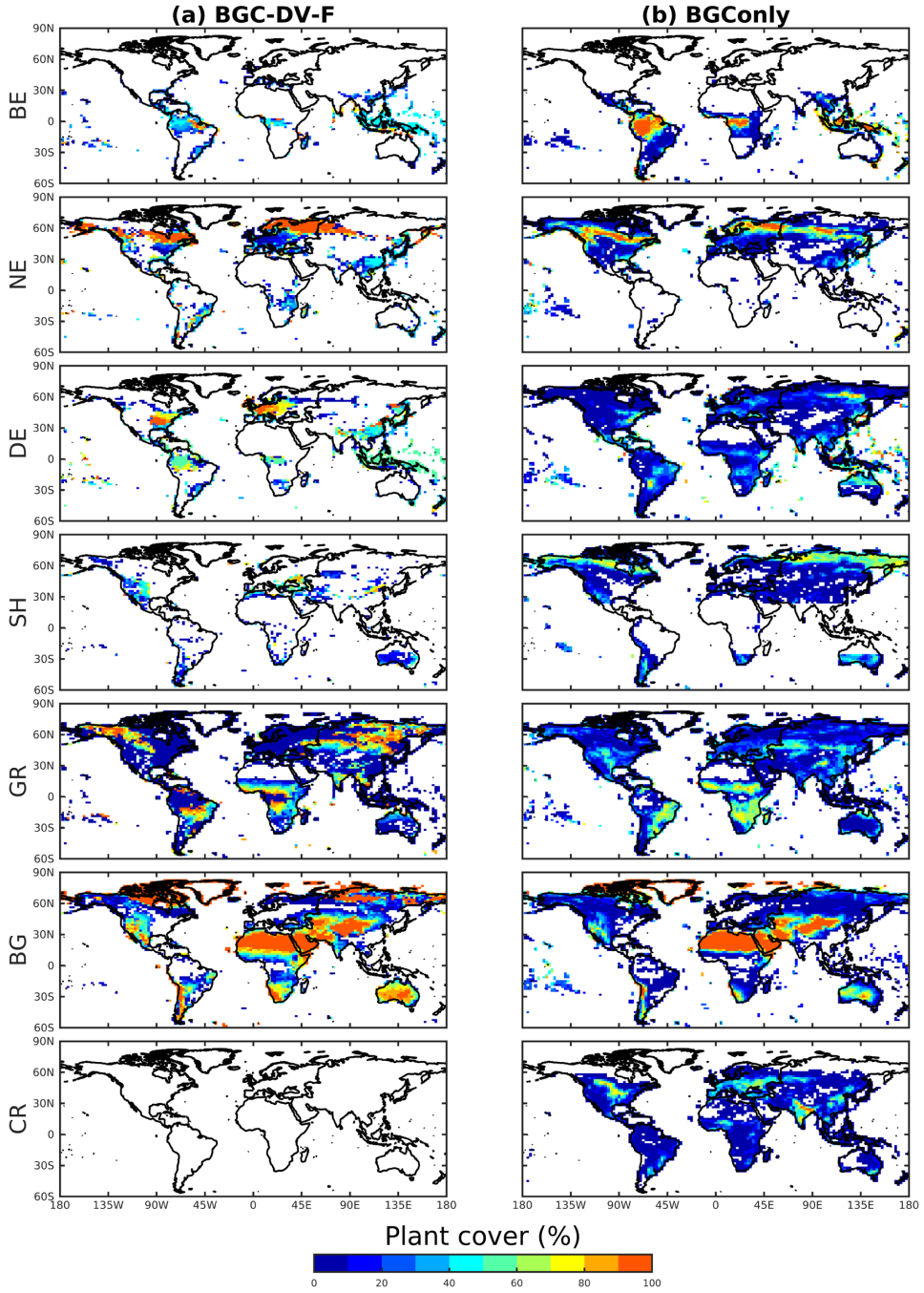

Figure 3: Percentages of land cover type (bare ground (BE), grass (GR), shrub (SH), deciduous (DE), needleleaf evergreen (NE), and broadleaf evergreen (BE)) in BGC-DV-F and BGConly.

Geosci. Model Dev. Discuss., https://doi.org/10.5194/gmd-2018-231
Manuscript under review for journal Geosci. Model Dev.
Discussion started: 15 October 2018

Geoscientific Model Development Discussions

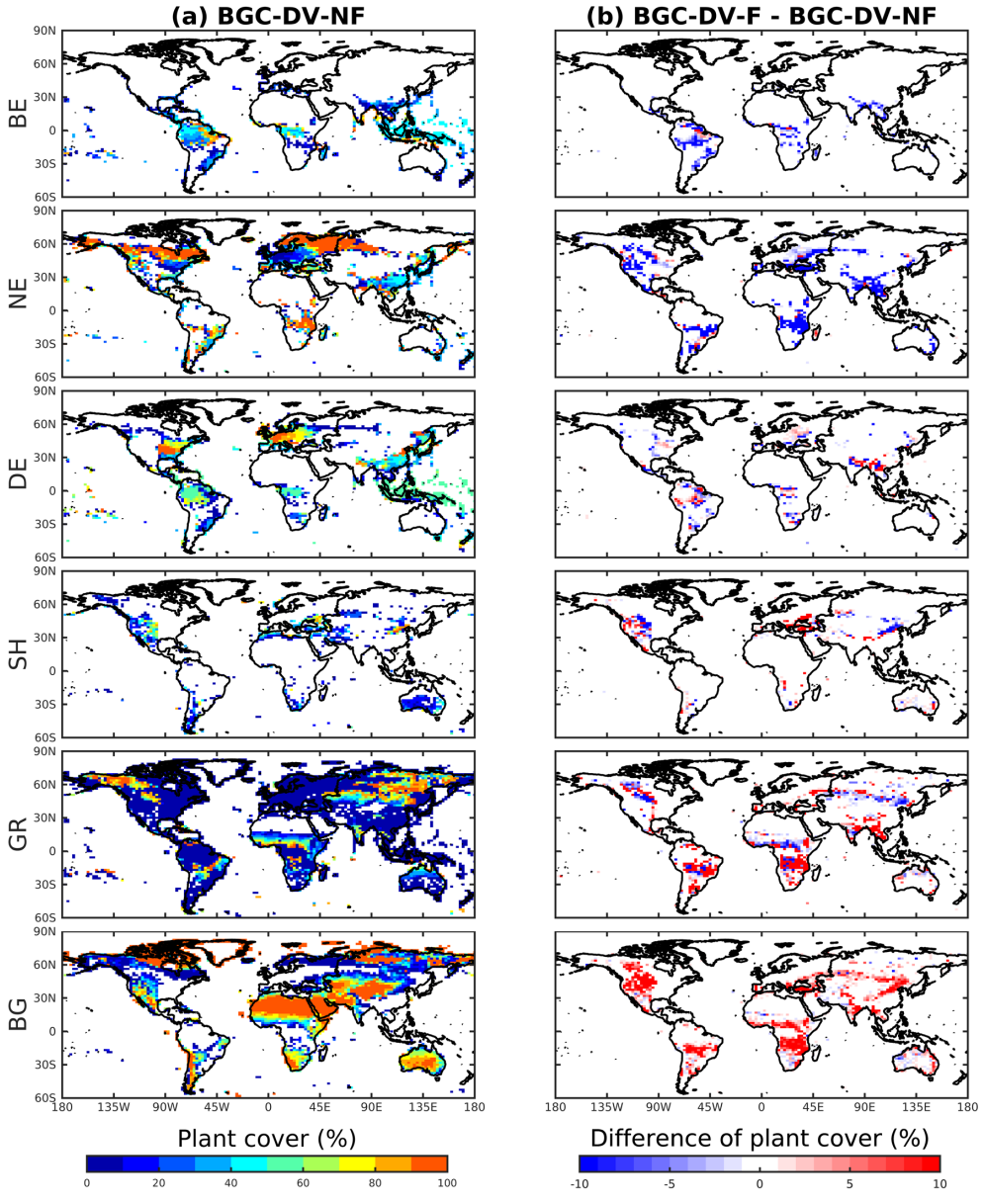

514

515 **Figure 4:** Percentages of land cover type (bare ground (BE), grass (GR), shrub (SH), deciduous (DE), needleleaf evergreen (NE),
516 and broadleaf evergreen (BE)) in BGC-DV-NF and differences in plant cover between BGC-DV-F and BGC-DV-NF.

Geosci. Model Dev. Discuss., https://doi.org/10.5194/gmd-2018-231
Manuscript under review for journal Geosci. Model Dev.
Discussion started: 15 October 2018

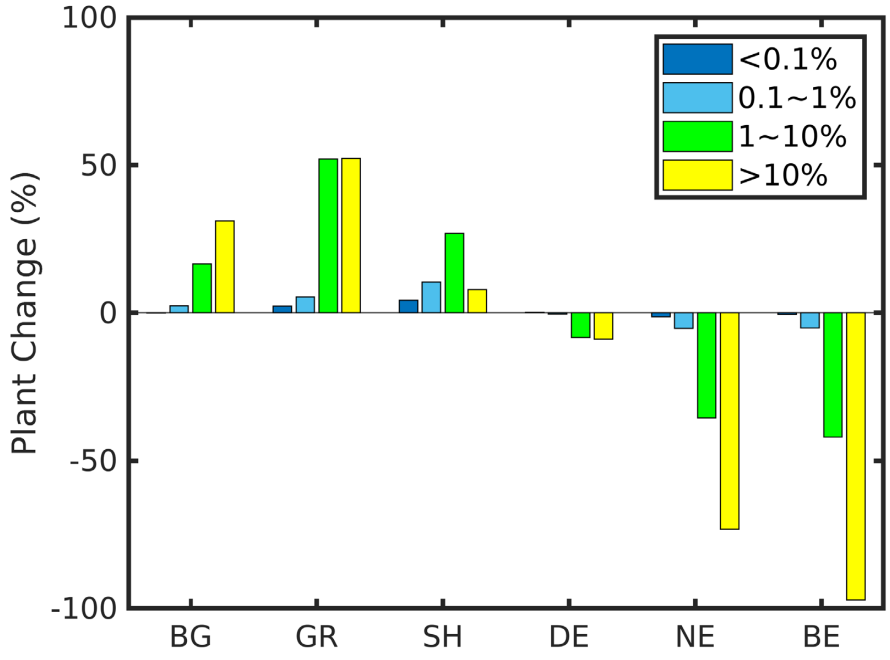

517

518 **Figure 5:** Changes in vegetation ratios for four burned area categories: under 0.1%, 0.1~1%, 1~10%, and greater than 10%.
519

Geosci. Model Dev. Discuss., https://doi.org/10.5194/gmd-2018-231
Manuscript under review for journal Geosci. Model Dev.
Discussion started: 15 October 2018

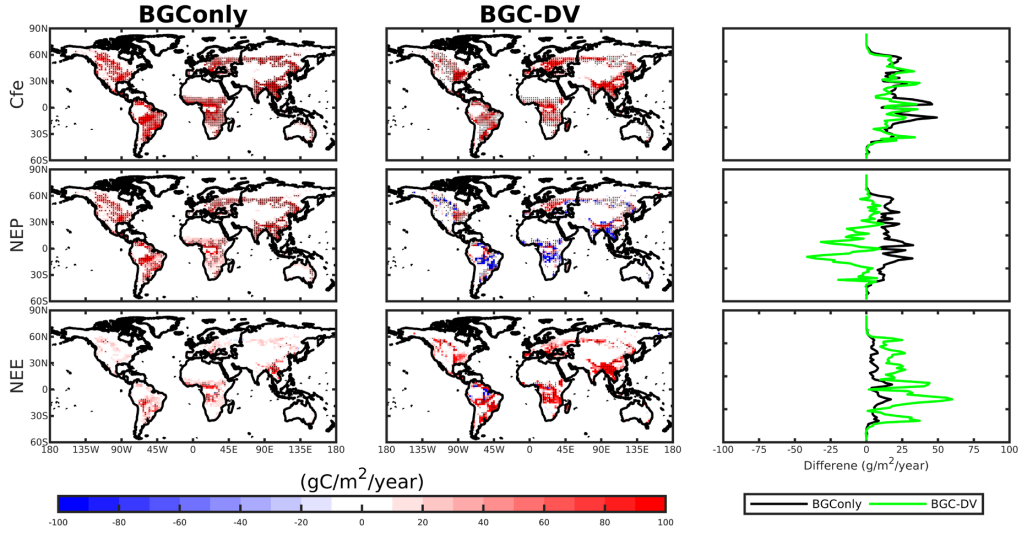

520
521 **Figure 6:** Differences in carbon emissions (Cfe), net ecological production (NEP), and net ecosystem exchange (NEE) due to fire
522 between BGC and BGC-DV. Hashed areas indicate that difference passed the Student's t-test at 0.05 significance level.
523 Latitudinal mean differences are plotted in far-right column.
524
525

Geosci. Model Dev. Discuss., https://doi.org/10.5194/gmd-2018-231
Manuscript under review for journal Geosci. Model Dev.
Discussion started: 15 October 2018

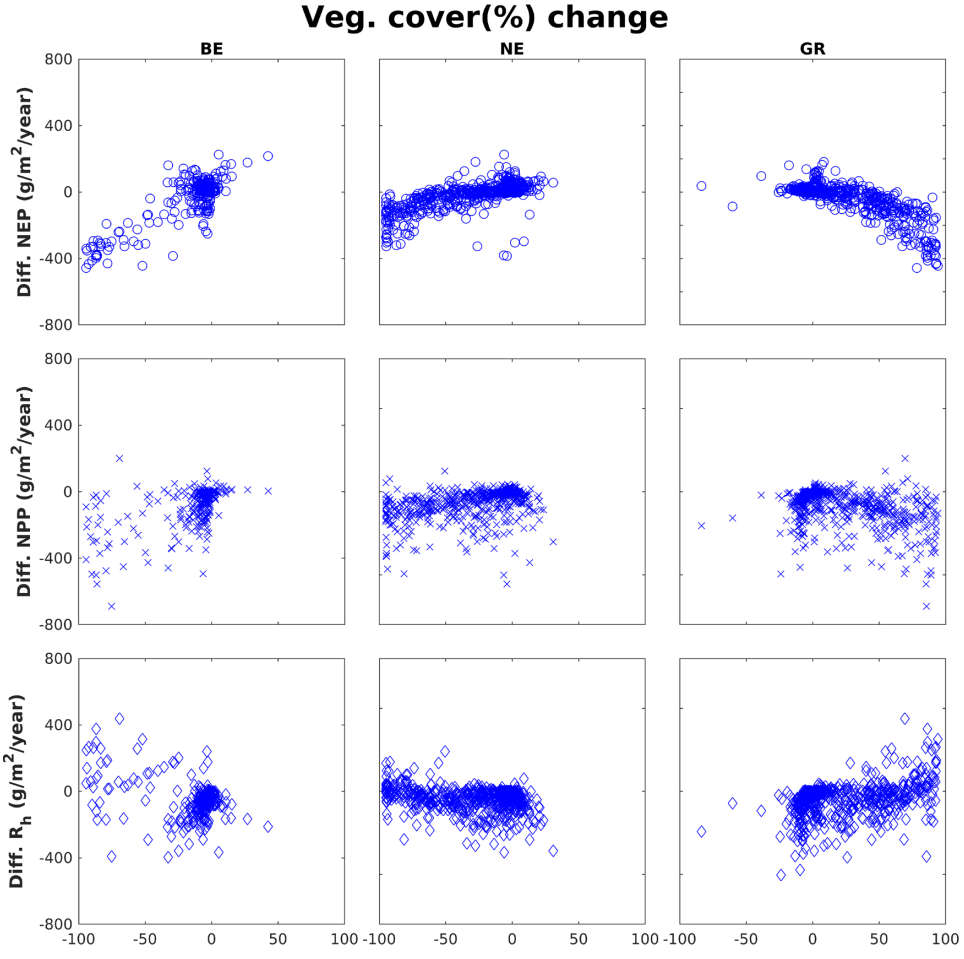

526

527 **Figure 7:** Response of differences (BGC-DV-F minus BGC-DV-NF) in NEP, NPP, and R_h to percentage changes in bare ground
528 (BE), needleleaf evergreen (NE), and grass (GR) vegetation types.

529

Geosci. Model Dev. Discuss., https://doi.org/10.5194/gmd-2018-231
Manuscript under review for journal Geosci. Model Dev.
Discussion started: 15 October 2018

Geoscientific Model Development Discussions
Open Access
EGU

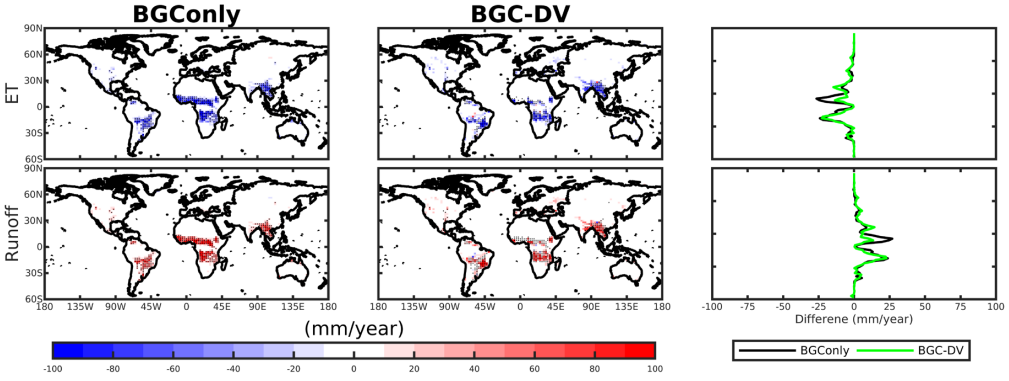

530
531 **Figure 8:** Same as Figure 6 but for water fluxes (evapotranspiration (ET) and runoff)
532

Geosci. Model Dev. Discuss., https://doi.org/10.5194/gmd-2018-231
Manuscript under review for journal Geosci. Model Dev.
Discussion started: 15 October 2018

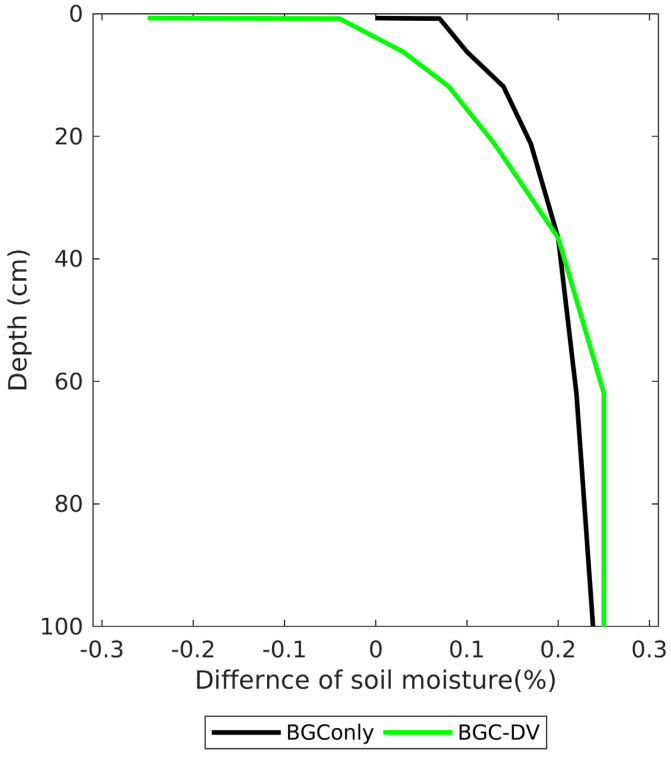

533

534 **Figure 9:** Difference in soil moisture (%) in BGConly and BGC-DV simulations.

535

Geosci. Model Dev. Discuss., https://doi.org/10.5194/gmd-2018-231
Manuscript under review for journal Geosci. Model Dev.
Discussion started: 15 October 2018

536 **Table 1:** Configurations of four experiments used in study.

Model option		Dynamic vegetation model	
		ON	OFF
Fire model	ON	BGC-DV-F	BGConly-F
	OFF	BGC-DV-NF	BGConly-NF

537
538

Geosci. Model Dev. Discuss., https://doi.org/10.5194/gmd-2018-231
Manuscript under review for journal Geosci. Model Dev.
Discussion started: 15 October 2018

539 **Table 2:** Percentage (%) land cover types (bare ground, grass, shrub, deciduous, needleleaf evergreen, and broadleaf evergreen)
540 in BGConly, BGC-DV-F, and BGC-DV-NF.

	BGConly	BGC-DV-F	BGC-DV-NF
Bare ground	28.17	41.21	38.66
Grass	20.13	21.25	16.53
Shrub	8.41	4.75	4.24
Deciduous	12.78	12.29	12.67
Needleleaf evergreen	9.96	14.73	20.54
Broadleaf evergreen	10.31	5.73	7.33
Crop	10.25	-	-

541
542

Geosci. Model Dev. Discuss., https://doi.org/10.5194/gmd-2018-231
Manuscript under review for journal Geosci. Model Dev.
Discussion started: 15 October 2018

543 **Table 3:** Annual means of carbon budget for GPP, NPP, Ra, Rh, NEP, NEE, and Cfe and differences (Fire on- Fire off) between
544 BGConly and BGC-DV simulations in Pg C yr-1. Asterisk (*) index indicates that difference in Fire on and Fire off simulations
545 passed the student's t test at $\alpha = 0.05$ significance level.

	BGConly			BGC-DV		
	Fire on	Fire off	Diff	Fire on	Fire off	Diff
C_{fe}	3.49	0.00	3.49*	2.98	0	2.98*
GPP	130.51	144.24	-13.73*	122.01	136.93	-14.92*
NPP	56.66	63.17	-6.51*	52.14	55.56	-3.42*
R_a	73.85	81.08	-7.23*	69.87	81.37	-11.50*
R_h	52.75	61.73	-8.98*	41.19	43.79	-2.60*
NEP	3.91	1.44	2.47*	13.65	14.67	-1.02*
NEE	-0.42	-1.44	1.02*	-5.27	-8.87	3.60*

546
547

Geosci. Model Dev. Discuss., https://doi.org/10.5194/gmd-2018-231
Manuscript under review for journal Geosci. Model Dev.
Discussion started: 15 October 2018

548 **Table 4:** Correlation coefficients between carbon fluxes (NEP, NPP, Rh) and percentage changes in vegetation cover for
549 broadleaf evergreen (BE), needleleaf evergreen (NE), deciduous (DE), shrub (SH), grass (GR), and bare ground (BG).

	BE	NE	DE	SH	GR	BG
NEP	0.84	0.68	0.34	-0.28	-0.80	-0.14
NPP	0.56	0.44	0.34	-0.30	-0.47	-0.35
R_h	-0.36	-0.17	-0.01	-0.13	0.27	-0.30

550
551

Geosci. Model Dev. Discuss., https://doi.org/10.5194/gmd-2018-231
Manuscript under review for journal Geosci. Model Dev.
Discussion started: 15 October 2018

552 **Table 5:** Same as Table 3, but for the water budgets of ground evaporation (GE), canopy evaporation (CE), canopy transpiration
553 (CE), evapotranspiration (ET), and total runoff (RO) in 103 km^3 yr^{-1}.

	BGConly			BGC-DV		
	Fire on	Fire off	Diff	Fire on	Fire off	Diff
GE	20.87	19.27	1.60*	23.29	19.61	3.68*
CE	15.71	16.39	-0.68*	15.62	16.88	-1.26*
CT	38.41	40.42	-2.01*	37.68	40.99	-3.31*
ET	74.99	76.08	-1.09*	76.59	77.48	-0.89*
RO	31.09	30.02	1.07*	29.51	28.64	0.87*

554
555

Geosci. Model Dev. Discuss., https://doi.org/10.5194/gmd-2018-231
Manuscript under review for journal Geosci. Model Dev.
Discussion started: 15 October 2018

556 **Table 6:** Same as Table 3, but for in LAI (m^2/m^2) and vegetation height(m).

	BGConly			BGC-DV		
	Fire on	Fire off	Diff	Fire on	Fire off	Diff
LAI	2.13	2.36	-0.23*	2.24	2.62	-0.38*
Height	7.05	7.45	-0.4*	6.03	7.76	-1.73*

557
558

Geosci. Model Dev. Discuss., https://doi.org/10.5194/gmd-2018-231
Manuscript under review for journal Geosci. Model Dev.
Discussion started: 15 October 2018

559 **Table 7:** Same as Table 3, but for soil moisture in (%) at each soil depth.

Depth	BGConly			BGC-DV		
	Fire on	Fire off	Diff	Fire on	Fire off	Diff
0.71 cm	21.22	21.22	0.00*	20.48	20.73	-0.25*
0.79 cm	23.22	23.15	0.07*	22.59	22.63	-0.04*
6.23 cm	23.24	23.14	0.10*	22.61	22.58	0.03*
11.89 cm	22.72	22.58	0.14*	22.14	22.06	0.08*
21.22 cm	22.37	22.2	0.17*	21.83	21.7	0.13*
36.61 cm	22.48	22.28	0.20*	21.98	21.78	0.2*
61.98 cm	22.57	22.35	0.22*	22.1	21.85	0.25*
103.8 cm	22.45	22.21	0.24*	21.95	21.7	0.25*

560